SURFACE INDUCTION HARDENING OF AXI-SYMMETRIC BODIES

*Jerzy BARGLIK, **Ivo DOLEŽEL, ***Martin ŠKOPEK, ****Bohuš ULRYCH
*Silesian University of Technology, Krasinskiego 8, 40 019 Katowice, Poland, barglik@mail.polsl.katowice.pl
**Institute of Electrical Engineering AS CR, Dolejškova 5, 182 02 Prague, Czech Republic, dolezel@iee.cas.cz
***Research Center "New Technologies", Universitní 8, 306 14 Plzeň, Czech Republic, skopekm@ntc.zcu.cz
****Faculty of Electrical Engineering UWB, Sady Pětatřicátníků 14, 306 14 Plzeň, Czech Republic, ulrych@kte.zcu.cz

SUMMARY

The paper deals with the mathematical and computer modelling of the surface induction hardening of axi-symmetric ferromagnetic bodies. The mathematical description of this non-stationary process consists of two second-order partial differential equations describing the heating of the body (time evolution of the electromagnetic and consequent temperature field) and a theoretically empirical algorithm for mapping the consequent cooling in various liquid media and hardening. The task is solved in the quasi-coupled formulation, with partial respecting the temperature dependencies of all important material parameters. The theoretical analysis is supplemented with several illustrative examples, whose solution was performed in co-operation of professional code QuickField and single-purpose user program package developed and written by the authors (as far as they know, no existing commercial program is able to map the complete process). The results showing the distribution of hardness as well as particular material components (martensite, ferrite, pearlite) within the hardened body are discussed.

Keywords: *induction heating, induction hardening, numerical solution, electromagnetic field, temperature field.*

1. INTRODUCTION

Induction hardening of ferromagnetic bodies belongs to widely used technological processes. The body is first heated to the austenitizing temperature and then rapidly cooled (by water spraying, merging the body into a cooling medium etc.) [1]. The result is harder but more fragile martensite structure.

Fig. 1 containing the unbalanced phase diagram of typical steel provides good information about the process of cooling and hardening. The temperature of all parts that are to be completely hardened should exceed temperature T_h that is by 30–50 °C higher than Ac_3. For example, fast cooling given by line 1 characterised by initial temperature $T_{start} > T_h$ leads to complete hardening of the material. On the other hand, lines 2 and 3 show slower cooling resulting in incomplete hardening (initial temperature T_{start} is lower than T_h or the resultant martensite structure contains also bainite, pearlite or ferrite).

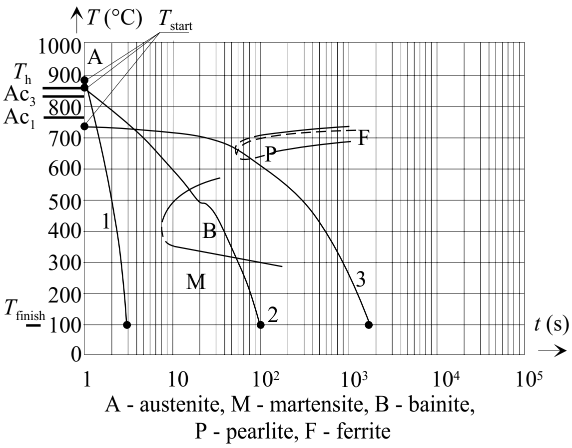

Fig. 1 Unbalanced phase diagram of typical steel

In general, induction heating may be strongly non-uniform process. The evolution of temperatures (Δt_1 being the time of heating) may differ from part to part of the body as indicated in Fig. 2. Sometimes it is desirable to wait some time Δt_2 in order to equalise the temperatures and obtain a chemically homogeneous single-phase austenite structure (but, of course, not in case of the surface hardening). The cooling of individual parts may also differ by velocity or, equivalently, by time Δt_3. The final distribution of hardness (in those parts where it is possible to speak about the full hardening, see Fig. 1) then strongly depends on time Δt_3.

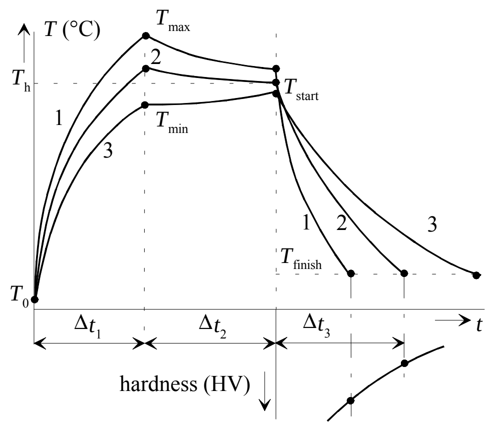

Fig. 2 Time evolution of the process

Mathematical and computer modelling of the described processes consists of two basic steps: the induction heating (Δt_1) itself and cooling (Δt_3) with eventual temperature equalisation (Δt_2). Various more or less sophisticated models of the induction heating may relatively reliably be solved by means of existing professional codes (sometimes supplemented with single-purpose user procedures). On the other hand, modelling of the temperature equalisation and particularly basic regimes of hardening (continual, by degrees etc.), resulting in computation of the distribution of hardness, is not a common business up to now.

The paper offers one of the possible ways of the complete solution of the surface induction hardening. Modelling of the induction heating consisting in the calculation of the coupled electromagnetic and non-stationary thermal fields starts from the simplified theoretical mathematical model of the process, while distribution of hardness is determined by means of specific theoretically empirical procedures based on using experimentally obtained data.

2. MATHEMATICAL MODEL OF THE PROBLEM AND ITS SOLUTION

The solved arrangement is depicted in Fig. 3. A ferromagnetic cylinder is heated in a cylindrical inductor carrying an alternating current of higher frequency. Geometry of the system as well as all electrical and material parameters are known (including their temperature dependencies). After reaching the necessary surface temperature of the cylinder the source is removed and the body is merged into a cooling medium.

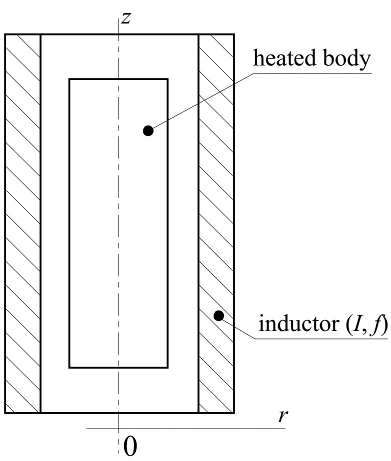

Fig. 3 The solved arrangement

The continuous mathematical model of the induction heating (first step of the process) is given by equations for distribution of the electromagnetic and temperature fields. The first equation [2] reads

$$\mathrm{rot}\left(\frac{1}{\mu}\mathrm{rot}\,\boldsymbol{A}\right)+\gamma\frac{\partial \boldsymbol{A}}{\partial t}=\boldsymbol{J}_{\mathrm{ext}}, \qquad (1)$$

where $\boldsymbol{A}$ denotes the vector potential, $\boldsymbol{J}_{\mathrm{ext}}$ the vector of the external current density in the inductor and μ and γ are the permeability and electrical conductivity of the material, respectively. The boundary conditions depend on the solved geometry. Usually, the Dirichlet condition is imposed along the axis of symmetry and distant artificial boundary, while the Neumann condition is mostly imposed along various planes of symmetry perpendicular to axis z.

The temperature field is described by well-known equation [3]

$$\mathrm{div}\left(\lambda\,\mathrm{grad}\,T\right)=\rho c\frac{\partial T}{\partial t}-w_{\mathrm{J}},\quad w_{\mathrm{J}}=\gamma\left(\frac{\partial \boldsymbol{A}}{\partial t}\right)^2, \qquad (2)$$

where T denotes the temperature and λ, ρ, c the thermal conductivity, specific mass and heat, respectively. Symbol w_{J} finally denotes the specific Joule losses within the body representing the source of heat. The boundary conditions along its surface should express both convection and radiation (higher temperatures are usually dealt with). The corresponding equation may be written as

$$-\lambda\cdot\frac{\partial T}{\partial n}=\alpha_{\mathrm{air}}\cdot\left(T-T_{\mathrm{ext}}\right)+\varepsilon_0\cdot C\cdot\left(T^4-T_{\mathrm{i}}^4\right), \qquad (3)$$

where $\varepsilon_0 = 5.67032\cdot10^{-8}$ W/m^2 K^4, α_{air} denotes the coefficient of the convective heat transfer, C the coefficient of emissivity, T_{ext} the temperature of the ambient air, T_{i} the temperature of the inductor and n the direction of the outward normal. The initial condition reads $T = T_0$. All material parameters and also coefficients α and C are generally non-linear functions of the temperature.

The second step (cooling in a liquid medium) is described by (2) in which term w_{J} vanishes. The boundary condition is now given by (3) without the second term on the right-hand side and with α for the cooling medium (that is now strongly temperature-dependent quantity). The resultant field of hardness is then determined in accordance with rules given in the preceding paragraphs.

Discretisation of the continuous model provided numerical algorithms for both induction heating and consequent cooling.

The process of induction heating was solved as a quasi-coupled problem [4] with partial respecting the temperature dependencies of the material parameters. The computations have been carried out by combination of code QuickField [5] (electromagnetic field) and user program TEMP_K1 (temperature field) based on combination of the Finite Difference Method and Method of Elementary Balances [6]. The algorithm consists of the following steps:

a) Choice of the starting temperature $T = T_0$ and determination of corresponding values of the material parameters (μ, γ, c, ρ, λ) and also coefficients α and C. Choice of time step Δt.
b) Solution of (1) and determination of distribution of the Joule losses w_{J}.
c) Computation of the time evolution of temperature field (2) up to time $t + \Delta t$ and modification of values of the material parameters with respect to actual temperature T.
d) Return to point b).

Steps b) – d) are repeated until temperature along the surface reaches the required value. The value of Δt has to be selected carefully and its choice should be verified by checking the convergence of solution and by its comparison with the accuracy required.

Solution of the process of cooling the body is somewhat simpler. The program has only to map the time evolution of the temperature at each node for assigning it its final structure (martensite, ferrite, pearlite or their mixtures) and corresponding hardness (if there is possible to speak about it). The crucial problem of cooling in liquids (water, oil, special hardening solutions etc. [7]) is, however, determining the temperature dependence of coefficient α. This dependence is mostly strongly non-linear, depends on the surface temperature of the hardened body and is closely associated with different regimes of boil of the cooling medium along its surface.

As the theoretical approach in this respect is extremely complicated, function $\alpha = \alpha(T)$ has been found by means of an experimentally-computational procedure consisting of the following steps:

a) A cylinder, whose material, dimensions and particularly quality of its surface was comparable with similar properties of the hardened body, was heated and then cooled in a liquid quenchant. Measured was velocity v_c (°C/s) of its cooling as a function of temperature T.
b) Using balance equation

$$Q = \rho \cdot V \cdot c \cdot v_c(T) = \alpha(T) \cdot S \cdot (T - T_{ext}), \quad (4)$$

where Q denotes the heat transferred from the cylinder per unit time, V is its volume, ρ its specific mass, c specific heat, S its surface and T_{ext} the temperature of the quenchant (that is considered constant), we simply get

$$\alpha(T) = v_c(T) \cdot \frac{\rho \cdot V \cdot c}{S \cdot (T - T_{ext})}. \quad (5)$$

Note that even other quantities occurring in (5) (including the volume and surface of the body) may be functions of the temperature.

3. ILLUSTRATIVE EXAMPLE

The task is to determine the field of hardness in a steel cylinder manufactured from standard carbon steel 40H [8] (produced in Poland, 0.42% C, 0.65% Mn, 0.017% P, 0.029%S and 1.00% Cr) heated in a cylindrical inductor and cooled in various liquid media (water, water-polymer medium called Polyhartenol, transformer oil and hardening oil 0H-70). The system consisting of the inductor and cylinder is axi-symmetric. Given are the following input data:

- Geometry of the cylinder: diameter d = 0.0125 m, length l = 0.060 m.
- Relative magnetic permeability μ_r of the steel is a function of the module of magnetic flux density $\boldsymbol{B}$ and temperature T. The dependence $\mu_r = \mu_r(|\boldsymbol{B}|)$ for steel 40H (for T = 0 °C) is depicted in Fig. 4. The general dependence of this quantity on field $|\boldsymbol{B}|$ and temperature T is considered as

$$\mu_r(|\boldsymbol{B}|, T) = 1 + (\mu_r(|\boldsymbol{B}|, 0) - 1) \cdot \varphi(T), \quad (6)$$

where $\varphi(T)$ (satisfying conditions $\varphi(0) = 1$ and $\varphi(T_c) = 0$, T_c being the Curie temperature) is depicted in Fig. 5.

- Other physical parameters of the cylinder (electrical conductivity, thermal conductivity and heat capacity) are depicted in Figs. 6 and 7.
- The inductor is a cylindrical coil wound from Cu conductor, with inner diameter 0.0185 m, outer diameter 0.0245 m and length 0.080 m.
- Parameters of the feeding current (current density J_{ext} = 48 A/mm^2, f = 10000 Hz) satisfy the condition that the time of heating does not exceed t_{stop} = 10 s.
- Starting temperature T_0 for induction heating as well as temperature T_{ext} of the surrounding air is 20 °C, α_{air} = 20 W/m^2 °C, C = 0.25.
- Ac_1 = 755 °C, Ac_3 = 790 °C, T_h = 840 °C and final temperature after cooling T_{finish} < 100 °C.
- The skin effect in the field coil is not taken into account.

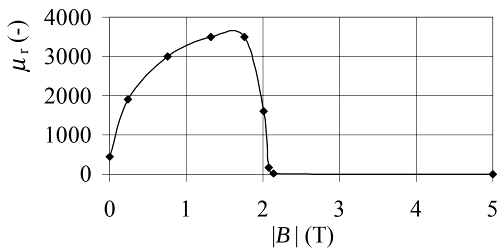

Fig. 4 $\mu_r = \mu_r(|\boldsymbol{B}|,0)$ for steel 40H at T = 0 °C

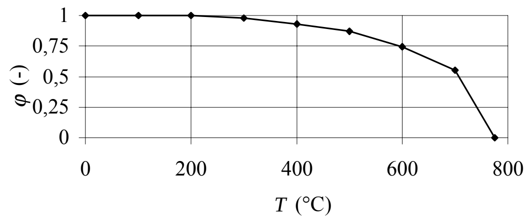

Fig. 5 Function $\varphi = \varphi(T)$ for correction of permeability μ_r for steel 40H

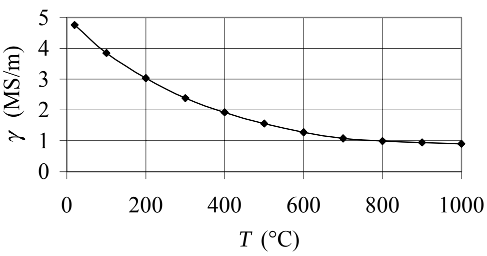

Fig. 6 Temperature dependence of electrical conductivity γ for steel 40H

Evaluation of the process of induction heating represents an open boundary problem. An artificial boundary was, therefore, introduced at a sufficient distance from the system characterised by the Dirichlet condition for vector potential $\boldsymbol{A}$ (Fig. 8).

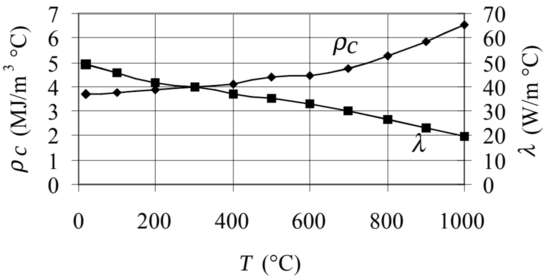

Fig. 7 Temperature dependence of thermal conductivity λ and heat capacity ρc for steel 40H

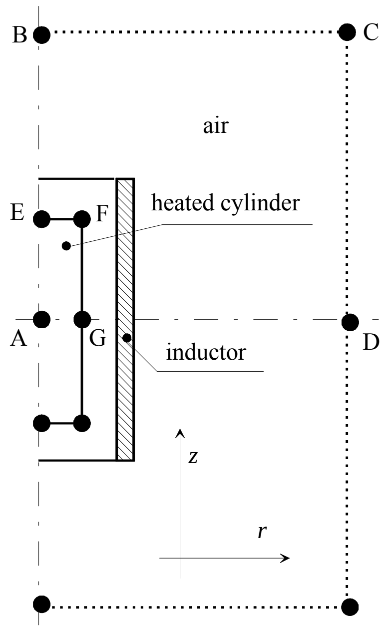

Fig. 8 The arrangement with artificial boundary ABCD

Because of symmetry the 2D electromagnetic field is solved only within area ABCDA. The boundary conditions along its respective parts read:

- ABCD: $\boldsymbol{A} = \boldsymbol{0}$,
- DA: $\dfrac{\partial \boldsymbol{A}}{\partial n} = \boldsymbol{0}$, (7)
- Initial condition: $\boldsymbol{A}_{t=0} = \boldsymbol{0}$.

Similarly, the temperature field is solved within area AGFEA (surface of the heated cylinder). Here the general boundary conditions read:

- EFG: see Eq. (3)
- GAE: $\dfrac{\partial T}{\partial n} = 0$, (8)
- Initial condition for heating: $T_{t=0} = T_0$.

The numerical solution was carried out by procedures mentioned in the previous paragraphs. The discretisation mesh constructed for computation of the electromagnetic field had about 22000 nodes, while the rectangular grid covering the cross-section of the heated cylinder for the thermal calculations only several hundred nodes. The test on stability showed that the calculations are stable for any time step $\Delta t \le 0.01$ s.

Fig. 9 shows the time evolution of temperature T in the course of the induction heating (Δt_1 = 10 s) at the "hottest" point G and the "coldest" point E (see Fig. 8) and Fig. 10 the histogram of the resultant temperatures after heating over plane AEFGA.

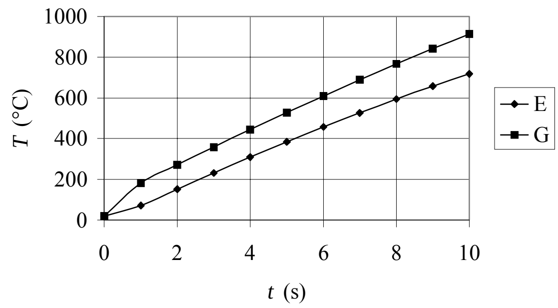

Fig. 9 Time evolution of temperature T at "hottest" point G and "coldest" point E

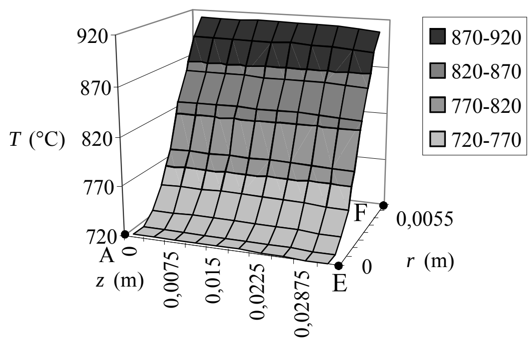

Fig. 10 Histogram of the distribution of temperature T over rectangle AEFGA (Fig. 8) after heating Δt_1

Interval Δt_2 necessary for removing the source and merging the body into cooling medium is considered small (several seconds) and its influence on the temperature distribution in the body was not respected (even when it is almost no complication). A lot of previous experience shows, however, that spontaneous cooling in the air is very slow and the surface temperatures may change only by few degrees within this period.

Obviously, temperature T_{h} before cooling is exceeded only in the surface layers of the cylinder. Its internal parts are substantially colder, after cooling remain unhardened and their structure consists of a mixture of the martensite, ferrite and pearlite.

Of crucial importance for correct quantification of the process of cooling is the knowledge of the temperature-dependent characteristics of the particular liquid media (velocity of cooling, time of cooling and coefficient α). These dependencies have been determined from sophisticated experiments carried out at the Silesian University of Technology, Katowice, Poland. One of them, the temperature dependence of coefficient α is depicted in Fig. 11.

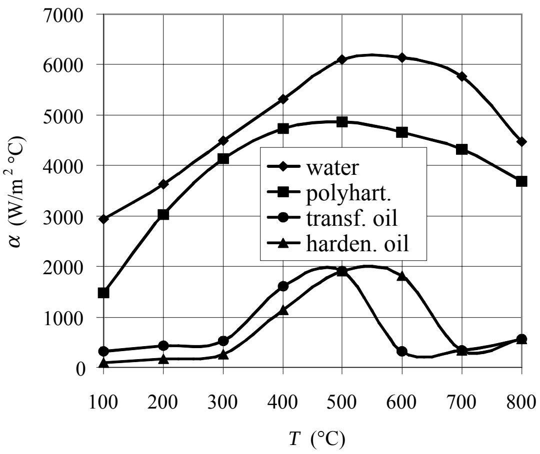

Fig. 11 Function $\alpha = \alpha(T)$ for the specified quenchants

It is obvious that the quenchant with the highest velocity of cooling is water followed by Polyhartenol. In both these cases the surface hardness reaches relatively high values, while in case of transformer oil or hardening oil 0H-70 its values can be unacceptably low.

The dependence of hardness for material 40H on the time of cooling (Δt_3) is depicted in Fig. 12.

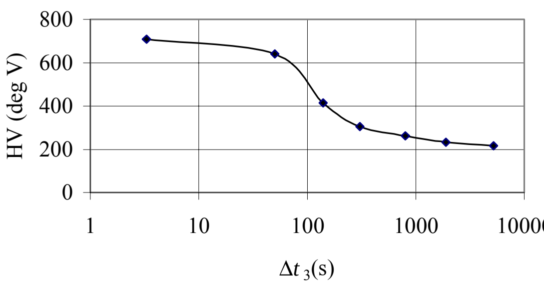

Fig. 12 Hardness HV as a function of time Δt_3 of hardening

Figs. 13 and 14 show the time decrease of the temperature at points A, E, G, F (see Fig. 8) during cooling the cylinder in water and the histogram of the final distribution of temperature after Δt_3 = 20 s over the rectangle specified by the same points.

Figs. 15 and 16 finally show the distribution of hardness (at places with the complete hardening) after cooling in selected quenchants (water and transformer oil). It is obvious that the highest hardness is reached after cooling in water. On the other hand, faster cooling may lead to internal stresses in the body, which are much lower at slower cooling in the transformer or hardening oil.

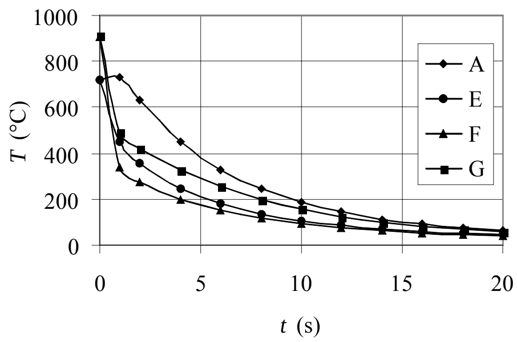

Fig. 13 Decrease of the temperature at the selected points of the cylinder (cooling in water)

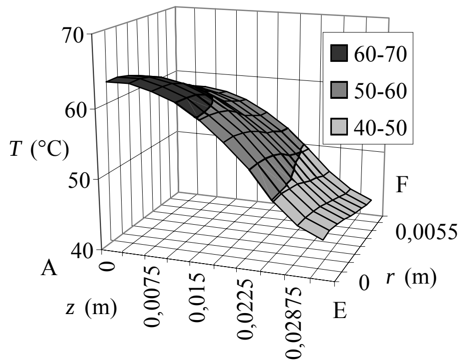

Fig. 14 Final distribution of the temperature over rectangle AEFGA after Δt_3 = 20 s (cooling in water)

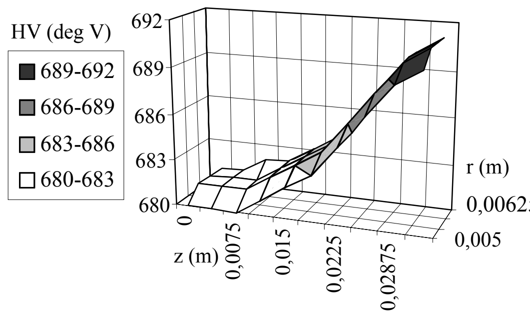

Fig. 15 The final distribution of hardness (in degrees of Vickers) in the body after cooling in water

4. CONCLUSION

The paper presents a methodology of the mathematical and computer modelling of the surface induction hardening. Solution to this multidisciplinary task seems to be feasible, however, in case of processing permeable materials some obstacles have to be overcome. The most serious problem consists in computation of the time evolution of the electromagnetic field (stiff system matrix, whose properties lead to extremely demanding time integration). In order to avoid this complication, only the average saturation in each element has been taken into account.

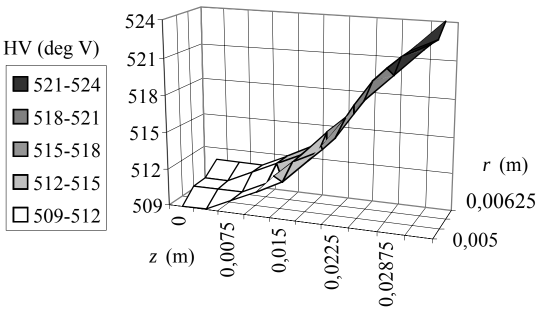

Fig. 16 Final distribution of hardness (in degrees of Vickers) after cooling in the transformer oil

Another problem is with necessary input data. Accuracy of computations strongly depends on the quality of experimentally obtained temperature-dependent material characteristics. Much more information is needed particularly in the domain of various metallurgic processes and properties of quenchants. Detailed knowledge of permeability μ_r as a function of the module of magnetic flux density $|\boldsymbol{B}|$ and temperature T would also surely contribute to higher quality of the results.

Nevertheless, the first results (for example [9] and [10]) are in a good accordance with experiments performed at the Silesian University of Technology in Katowice, Poland. Planned is further improvement of the computation procedures (increase of their robustness, stability and velocity) as well as their verification by comparison with other measurements.

ACKNOWLEDGEMENT

Financial support of the Grant Agency of the Czech Republic (project No. 102/01/0184) and Polish Science Research Committee (project No. 7T08603716) is highly acknowledged.

REFERENCES

[1] C. R. Brooks: The metallurgy of induction surface hardening. Advanced Materials & Processes, Dec. 2000, pp. H19–H23.
[2] J. A. Stratton: Electromagnetic Theory. McGraw-Hill Book Comp., 1941.
[3] P. J. Schneider: Conduction Heat Transfer. Addison-Wesley Pub Comp. Cambridge, Mass, 1955.
[4] K. Kurek, R. Przylucki, B. Ulrych: Induction heating as coupled or non-coupled electromagnetic and thermal problems. Acta Technica CSAV, Vol. 42, 1997, pp. 269–280.
[5] www.quickfield.com (March 2001).
[6] E. Vitásek: Numerical Methods. SNTL Prague, 1987, in Czech.
[7] Industrial quenching oils - determination of cooling characteristics - nickel alloy probe test method. ISO Ref. Number 9950, 1995.
[8] Characteristics of steels. Internal report of the Institute of Metallurgy, Silesian University of Technology, Gliwice, Poland, 1991, pp. 404, in Polish.
[9] J. Barglik, I. Doležel, K. Ducki, B. Ulrych: Induction heating and consequent hardening of a ferromagnetic cylinder in various cooling media. Proceedings of SPETO 01, Ustron, Poland, May 2001, pp. 269–280.
[10] J. Barglik, I. Doležel, K. Ducki, B. Ulrych: Mathematical and computer modelling of induction heating and consequent hardening of circular saw. Proceedings of ISEF, Cracow, Poland, September 2001, pp. 513–518.

BIOGRAPHY

Dr. Jerzy Barglik (1949) has been working since 1973 at the Department of Electrotechnology of the Silesian University of Technology in Katowice, Poland. He is specialised in electromagnetic field calculations in induction heaters and other electroheating devices. Author or co-author of about 90 papers. He is strongly involved in international collaboration with several European and American universities.

Prof. Ivo Doležel (1949) obtained his Eng. degree from the Faculty of Electrical Engineering (Czech Technical University in Prague) in 1973 and since then he has been working in the Institute of Electrical Engineering of the Academy of Sciences of the Czech Republic. He is aimed mainly at electromagnetic fields and coupled problems in heavy current applications. Author or co-author of more than 150 papers. Wide tutorial activities at Faculties of Electrical Engineering in Prague and Plzeň.

Martin Škopek (1975) finished his studies at the Faculty of Electrical Engineering of the University of West Bohemia in Plzeň in 1998. He first worked as a doctoral student in the Department of Theory of Electrical Engineering and since 2000 he has been working at the National Research Centre "New Technologies in Plzeň". He is focused on coupled problems and SW used for their processing. Author or co-author of about 40 papers.

Assoc. Prof. Bohuš Ulrych (1937) has been working for a long time in the Department of Theory of Electrical Engineering at the Faculty of Electrical Engineering of UWB in Plzeň. His professional interests are aimed at modern numerical methods of solution of electromagnetic and coupled problems. Author and co-author of about 130 papers and several textbooks. Author of a lot of user's SW for calculation of electromagnetic fields and coupled problems.